

A stretchable temperature sensor based on elastically buckled thin film devices on elastomeric substrates

Cunjiang Yu, Ziyu Wang, Hongyu Yu, and Hanqing Jiang

Citation: [Applied Physics Letters](#) **95**, 141912 (2009); doi: 10.1063/1.3243692

View online: <http://dx.doi.org/10.1063/1.3243692>

View Table of Contents: <http://scitation.aip.org/content/aip/journal/apl/95/14?ver=pdfcov>

Published by the [AIP Publishing](#)

Articles you may be interested in

[Steady heat conduction-based thermal conductivity measurement of single walled carbon nanotubes thin film using a micropipette thermal sensor](#)

Rev. Sci. Instrum. **84**, 034901 (2013); 10.1063/1.4792841

[Buckling transitions of an elastic filament in a viscous stagnation point flow](#)

Phys. Fluids **24**, 123601 (2012); 10.1063/1.4771606

[Note: Response characteristics of the sensor based on LaF3 thin film to different humidified gases](#)

Rev. Sci. Instrum. **83**, 056103 (2012); 10.1063/1.4718358

[Note: Epitaxial ruby thin film based photonic sensor for temperature measurement](#)

Rev. Sci. Instrum. **82**, 066106 (2011); 10.1063/1.3606443

[Buckling modes of elastic thin films on elastic substrates](#)

Appl. Phys. Lett. **90**, 151902 (2007); 10.1063/1.2720759

The advertisement features a red and white color scheme. On the left, there is a red button with the text 'View video demo >'. To the right of the button, the text reads 'Confidently measure down to 0.01 fA and up to 10 PΩ' in red, followed by 'Keysight B2980A Series Picoammeters/Electrometers' in black. On the right side of the advertisement, there is an image of a Keysight B2980A Series Picoammeter/Electrometer device and the Keysight Technologies logo.

A stretchable temperature sensor based on elastically buckled thin film devices on elastomeric substrates

Cunjiang Yu,¹ Ziyu Wang,^{2,3} Hongyu Yu,^{2,4,a)} and Hanqing Jiang^{1,b)}

¹*School of Mechanical, Aerospace, Chemical and Materials Engineering, Arizona State University, Tempe, Arizona 85287, USA*

²*School of Electrical, Computer and Energy Engineering, Arizona State University, Tempe, Arizona 85287, USA*

³*Department of Physics, Wuhan University, Wuhan 430072, People's Republic of China*

⁴*School of Earth and Space Exploration, Arizona State University, Tempe, Arizona 85287, USA*

(Received 5 June 2009; accepted 14 September 2009; published online 8 October 2009)

Stretchable electronics and sensors have been attracting significant attention due to their unique characteristics and wide applications. This letter presents a prototype of a fully stretchable temperature sensor on an elastomeric substrate. The sensor was fabricated on a silicon-on-insulator wafer and then transferred to a prestrained elastomeric polydimethylsiloxane substrate. Releasing the prestrain on the substrates led to the formation of the microscale, periodic, wavy geometries of the sensor. The thin wavy sensor device can be reversibly bent and stretched up to 30% strain without any damage or performance degradation. A theoretical analysis was also developed to estimate the wavy profile. © 2009 American Institute of Physics. [doi:10.1063/1.3243692]

There is a strong desire to substitute conventional electronics on rigid substrates with mechanically flexible or stretchable equivalents that are almost non-noticeable to users. Flexible electronic devices, such as sensitive skins,¹⁻³ flexible flow sensors,^{4,5} and flexible thin film transistors^{6,7} supported by flexible materials while maintaining high performance have been developed. However, these devices provide limited stretchability or bendability;⁸ the devices fail when conformed or mounted to large curvatures or undergo large mechanical deformations, as shown in Table I. There is a definite need to develop flexible and highly stretchable devices that survive under large deformations. This letter reports a design and fabrication method, which integrates elastomeric substrates with ultrathin stiff film devices on top to overcome the limitations. The fabricated sensors can be reversibly stretched and compressed up to 30% mechanical strain without any fracture or sensor performance degradation.

Figure 1 illustrates the fabrication flow of the stretchable temperature sensor. The fabrication began with spinning and patterning photoresist (AZ 4330, AZ Electronic Materials USA Corp.) using standard lithography process on a silicon-on-insulator (SOI) wafer (400 nm thick box layer, 340 nm thick single crystal silicon film). A thermistor was fabricated by sputter deposition of a thin Cr/Au layer of 5 nm/20 nm and patterned by lift-off process. Another Cr/Au layer (5 nm/200 nm) served as electrodes was then deposited and patterned using the same method. Silicon ribbons (6 mm × 400 μm) were patterned from the thin single crystal silicon on top the oxide layer, using reactive ion etching. The silicon ribbons function as both supporting layer for the thermistor and the adhesive layer with the elastomeric substrates. The oxide box layer beneath the silicon ribbons was then etched in concentrated hydrofluoric acid (49%), releasing the silicon film with the thermistor anchored at two ends. After

air drying, the thin devices rested on the silicon substrate.

Transfer steps are employed to form the buckled devices.⁸⁻¹⁰ A 1 cm thick elastomeric polydimethylsiloxane (PDMS) stamp (Sylgard 184, Dow Corning, Inc., mixing ratio of base: curing agent is 5:1 by weight) was brought to slightly contact with the wafer. The fabricated devices stuck on the PDMS stamp by the van der Waals interactions were quickly peeled off from the SOI wafer. Another 1 mm thick PDMS slab (mixing ratio of base: curing agent is 10:1 by weight) is stretched by a custom made stage through which the desired strain level could be achieved, and exposed by a ultraviolet/ozone (UVO) light (BHK, Inc.) for 3 min to form a chemically activated surface that can bond with silicon or silicon oxide.^{8,9} The devices on the PDMS stamp (mixing ratio 5:1) are finally transferred to the prestrained PDMS slab (mixing ratio 10:1) along the direction of the prestrain and slowly peeling off the PDMS stamp.^{10,11} The prestrained and UVO treated PDMS slab with transferred thin devices was heated in an oven at 90 °C for 5 min to enhance the chemical bonding reaction. Releasing the prestrain in PDMS substrates led to the spontaneous formation of periodically buckled patterns due to the mechanical competition between the relatively stiff films and the compliant PDMS substrate.

TABLE I. Limited stretchability of various flexible devices.

Flexible devices	Flexible devices	Stretchability
Sensitive skin ^{a,c}	Functional devices embedded into flexible substrates	
Flexible sensors ^{d,e}	Isolated functional devices printed or built on flexible substrates	<1%
Flexible TFTs ^{f,g}	TFTs from thick substrate glued onto flexible substrates	

^aReference 1.

^bReference 2.

^cReference 3.

^dReference 4.

^eReference 5.

^fReference 6.

^gReference 7.

^{a)}Electronic mail: hongyu.yu@asu.edu.

^{b)}Electronic mail: hanqing.jiang@asu.edu.

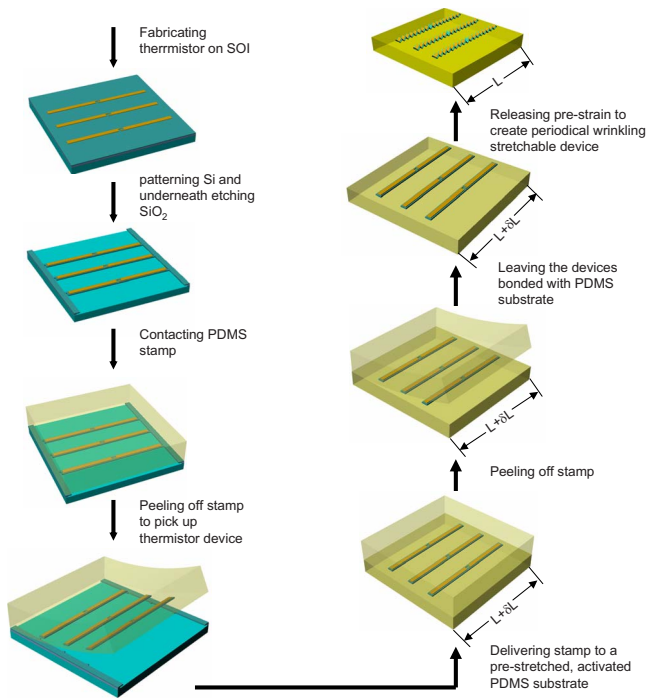
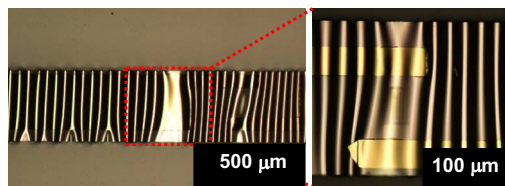


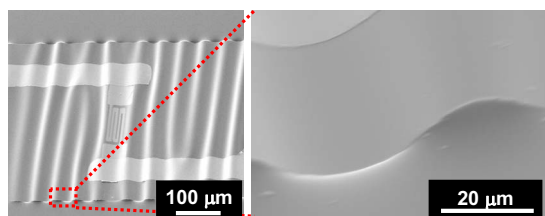
FIG. 1. (Color online) Schematic illustration of the fabrication process.

Figure 2(a) shows the images of the buckled devices by 10% prestrain. The buckling wavelength and amplitude are 81.6 and 8.5 μm , respectively. At the sensing element region, the regular wavy shape was disturbed due to the changes of boundary condition and structure layer thickness, which, however, has no effect on sensors' performance as to be shown. Figure 2(b) is a tilted scanning electron microscopy (SEM) image that reveals that the surface of the PDMS substrate fluctuates in the same manner as the buckled thin film, which indicates strong bonding between silicon and PDMS.¹² Previous experiments even shown that the interface remains intact even the silicon fails; thus, the thin films do not form self-curling after peeled off from the SOI substrates.

The buckling profile plays an important role in the stretchability of the thin film device/substrate system. In the following analysis, a nonlinear buckling based on the energy



(a)



(b)

FIG. 2. (Color online) (a) Stretchable sensors on top of a PDMS substrate with periodically buckled patterns. (b) Tilted SEM view of stretchable temperature sensor and the interface between the buckled sensor and PDMS.

method is presented to study the buckling behavior.¹²

The total energy, U_{tot} , consists of three parts, the bending energy U_b , due to thin film buckling, the membrane energy U_m , in the thin film device, and substrate energy U_s . The buckling profile can be expressed as a sinusoidal form as $w=A \cos(2\pi x/\lambda)$, where A and λ are the buckling amplitude and wavelength to be determined; x is the prestrain direction. Since the thickness of Cr layer (5 nm) is much thinner than the other two layers (Si layer 340 nm and Au layer 200 nm), a double-layer model was used in the following analysis. The bending energy U_b in the thin film device can be obtained from the buckling profile and the effective bending rigidity of the composite beam $\alpha \bar{E}_{\text{Si}} h_{\text{Si}}^3/12$ as $U_b = [1/(1+\epsilon_{\text{pre}})^3 \lambda] \int_0^\lambda (1/2) (\bar{E}_{\text{Si}} h_{\text{Si}}^3/12) \alpha (d^2 w/dx^2)^2 dx = [\bar{E}_{\text{Si}} h_{\text{Si}}^3 A^2 \pi^4/3(1+\epsilon_{\text{pre}})^3 \lambda^4] \alpha$, where a nondimensional parameter $\alpha = \{1/[1+(\bar{E}_{\text{Au}}/\bar{E}_{\text{Si}})(h_{\text{Au}}/h_{\text{Si}})]\} [1+4(\bar{E}_{\text{Au}}/\bar{E}_{\text{Si}}) \times (h_{\text{Au}}/h_{\text{Si}}) + 6(\bar{E}_{\text{Au}}/\bar{E}_{\text{Si}})(h_{\text{Au}}/h_{\text{Si}})^2 + 4(\bar{E}_{\text{Au}}/\bar{E}_{\text{Si}})(h_{\text{Au}}/h_{\text{Si}})^3 + (\bar{E}_{\text{Au}}/\bar{E}_{\text{Si}})^2 (h_{\text{Au}}/h_{\text{Si}})^4]$ is introduced to express the shift of the neutral plane, h is the film thickness, $\bar{E} = E/(1-\nu^2)$, E and ν are the plane-strain modulus, Young's modulus and Poisson's ratio, respectively, and the subscripts refer to Au and Si thin films. The membrane energy in the thin film device is obtained by the effective tension stiffness $h_{\text{Si}} \bar{E}_{\text{Si}} + h_{\text{Au}} \bar{E}_{\text{Au}} = h_{\text{Si}} \bar{E}_{\text{Si}} [1 + (\bar{E}_{\text{Au}}/\bar{E}_{\text{Si}})(h_{\text{Au}}/h_{\text{Si}})] = h_{\text{Si}} \bar{E}_{\text{Si}} \beta$ and membrane strain $\epsilon_{\text{mem}} = [A^2 \pi^2/\lambda^2 (1+\epsilon_{\text{pre}})^2] - [\epsilon_{\text{pre}}/(1+\epsilon_{\text{pre}})]$ as $U_m = [(1+\epsilon_{\text{pre}})/\lambda] \int_0^\lambda (1/2) h_{\text{Si}} \bar{E}_{\text{Si}} \beta \epsilon_{\text{mem}}^2 dx = (1/2) (1+\epsilon_{\text{pre}}) h_{\text{Si}} \bar{E}_{\text{Si}} \beta [A^2 \pi^2/\lambda^2 (1+\epsilon_{\text{pre}})^2 - [\epsilon_{\text{pre}}/(1+\epsilon_{\text{pre}})]]^2$. The substrate energy is given by $U_s = (\pi/3) (E_{\text{PDMS}} A^2/\lambda^2) [1 + (5/32)(\pi^2 A^2/\lambda^2)]$, where the PDMS substrate is considered incompressible.

Minimization of total energy U_{tot} with respect to the buckling amplitude A and wavelength λ , i.e., $\partial U_{\text{tot}}/\partial A = 0$, $\partial U_{\text{tot}}/\partial \lambda = 0$, gives

$$A = \begin{cases} h_{\text{Si}} \sqrt{\frac{\alpha}{\beta}} \sqrt{\frac{\epsilon_{\text{pre}}}{\epsilon_c} - 1} (1+\epsilon_{\text{pre}})^{-1/2} (1+\xi)^{-1/3}, & \epsilon_{\text{pre}} > \epsilon_c \\ 0, & \epsilon_{\text{pre}} < \epsilon_c, \end{cases} \quad (1)$$

$$\lambda = \frac{2\pi h_{\text{Si}}}{1+\epsilon_{\text{pre}}} \left(\frac{\bar{E}_{\text{Si}} \alpha}{3\bar{E}_{\text{PDMS}}} \right)^{1/3} (1+\xi)^{-1/3}, \quad (2)$$

where $\epsilon_c = (1/4)(3\bar{E}_{\text{PDMS}}/\bar{E}_{\text{Si}})^{2/3} (\alpha^{1/3}/\beta)$ is the critical strain for buckling, or the minimum strain needed to induce buckling, and $\xi = (5/32)\epsilon_{\text{pre}}(1+\epsilon_{\text{pre}})$. Using the following literature values^{8,13,14} for the mechanical properties ($E_{\text{Au}} = 69$ GPa, $\nu_{\text{Au}} = 0.43$, $E_{\text{Si}} = 130$ GPa, $\nu_{\text{Si}} = 0.3$, $E_{\text{PDMS}} = 2$ MPa) and the geometric parameters ($h_{\text{Au}} = 200$ nm, $h_{\text{Si}} = 340$ nm), with $\epsilon_{\text{pre}} = 10\%$, the amplitude and wavelength were calculated based on Eqs. (1) and (2) to be $A = 8.5$ μm and 80.8 μm , respectively, which agree very well with experimental data [Fig. 2(b)] without any parameter fitting.

When $\epsilon_{\text{pre}} > \epsilon_c$, the film buckles to release the strain; the membrane strain, ϵ_{mem} , has a magnitude almost equal to $-\epsilon_c$. The thin film peak strains ϵ_{peak} is the sum of membrane strain ϵ_{mem} and the strain induced by the buckled geometry. In most cases of practical interest, the strain associated with the buckled geometry is much larger than ϵ_{mem} . Thus, the peak strain of the film is fairly the bending strain due to

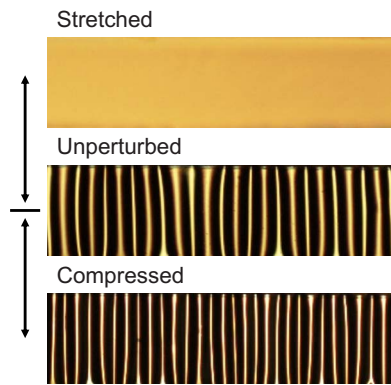


FIG. 3. (Color online) Optical images of stretchable temperature sensor on a PDMS substrate at -10% (top), 0% (middle) and 10% (bottom) applied strain.

buckling, which is much smaller than the prestrain. For example, in the case of $\varepsilon_{\text{pre}}=30\%$ the geometric parameters ($h_{\text{Au}}=200$ nm, $h_{\text{Si}}=340$ nm), the peak strain in silicon $\varepsilon_{\text{peak}}^{\text{Si}}$ is calculated to be only 1.65% , which does not reach the fracture strain of single crystal silicon ($\sim 2\%$).⁸ In fact, the silicon peak strain can be further reduced for thinner film even subjected to larger prestrain. This mechanical advantage provides an effective level of stretchability/compressibility in materials.

To experimentally demonstrate the stretchability, the stretchable temperature sensor device was mechanically stretched and compressed to limited (~ 100) cycles. No obvious cracks were observed, though microcracks might exist, which needs high resolution characterization. The mechanism is that the strain in the thin films is accommodated by changing the buckling amplitude and wavelength, thereby avoiding the substantial strains in the stiff film structures. Figure 3 shows optical images of the stretchable sensors subjected to 10% (top), 0% (middle) and -10% applied strains. It is observed that the wavelength is adjusted to response the applied strain, similar to accordion bellows. Once the applied strain reaches the prestrain, the buckled films are stretched flat and then fail. Thus, the stretchability is mainly determined by the prestrain on PDMS substrate, for given thin film geometries.

The functionality of the stretchable temperature sensor was studied. A stretchable sensor (formed by 30% prestrain) was stretched to flat (by 30% applied strain) at the room temperature and the electrical resistance was measured [Fig. 4(a)]. The constant electrical resistance indicates that the stretchability due to buckling does not affect the electrical resistance. The electrical resistance over a range of temperature under different applied strains was measured, as shown in Fig. 4(b). Since the deformation of the thin film and substrate is elastic, there is no hysteresis for the relation between resistance and strain; though, it is unknown if hysteresis exists for resistance/temperature, which needs to be further studied. There is no variation in the linear relation between electrical resistance and temperature when sensors were stretched or compressed for different strain levels. The slope, namely the thermal coefficient of resistance, given by the linear fitting agrees very well with that of the thermistors on flat rigid substrates.

In conclusion, temperature sensors fabricated by standard micromachining technology were integrated with elas-

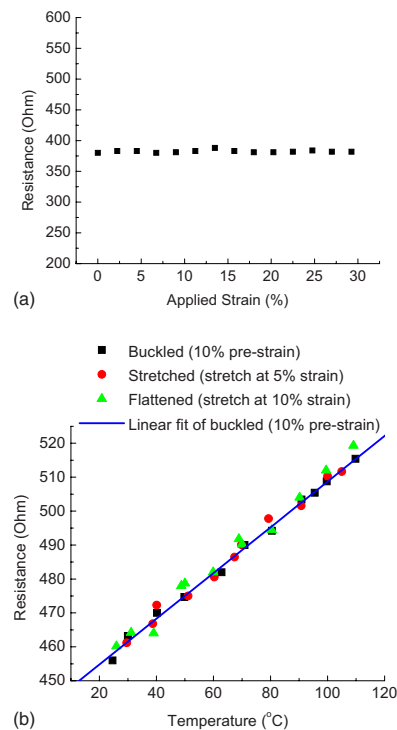


FIG. 4. (Color online) (a) Resistance of the stretchable sensor at room temperature during continuous stretch with the strain step of 2.25% up to 30% . (b) The electrical resistance vs temperature of a stretchable sensor with applied strain of 0 , 5 , and 10% .

tomeric substrate to achieve high stretchability for applications where large mechanical strain is induced or exists. The stretchability is realized by the periodically wavy structure supported by elastomeric substrates. The fabricated sensors can be stretched and compressed up to 30% with unchanged performance.

H.J. acknowledges the support from NSF (Grant No. CMMI-0700440). H.Y. acknowledges the financial support from ASU.

¹V. J. Lumelsky, M. S. Shur, and S. Wagner, *IEEE Sens. J.* **1**, 41 (2001).

²Y. Xu, Y. C. Tai, A. Huang, and C. M. Ho, *J. Microelectromech. Syst.* **12**, 740 (2003).

³Y. Xu, F. Jiang, S. Newbern, A. Huang, C. M. Ho, and Y. C. Tai, *Sens. Actuators, A* **105**, 321 (2003).

⁴H. Yu, L. Ai, M. Rouhanizadeh, D. Patel, E. S. Kim, and T. K. Hsiai, *J. Microelectromech. Syst.* **17**, 1178 (2008).

⁵R. Buchner, K. Froehner, C. Sosna, W. Benecke, and W. Lang, *J. Microelectromech. Syst.* **17**, 1114 (2008).

⁶H. C. Yuan, Z. Ma, M. M. Roberts, D. E. Savage, and M. G. Lagally, *J. Appl. Phys.* **100**, 013708 (2006).

⁷H. C. Yuan and Z. Ma, *Appl. Phys. Lett.* **89**, 212105 (2006).

⁸D. Y. Khang, H. Q. Jiang, Y. Huang, and J. A. Rogers, *Science* **311**, 208 (2006).

⁹Y. G. Sun, W. M. Choi, H. Q. Jiang, Y. G. Y. Huang, and J. A. Rogers, *Nat. Nanotechnol.* **1**, 201 (2006).

¹⁰J. Yoon, A. J. Baca, S. I. Park, P. Elvikis, J. B. Geddes III, L. F. Li, R. H. Kim, J. Xiao, S. Wang, T. H. Kim, M. J. Motala, B. Y. Ahn, E. B. Duoss, J. A. Lewis, R. G. Nuzzo, P. M. Ferrira, Y. Huang, A. Rockett and J. A. Rogers, *Nature (London)* **7**, 907 (2008).

¹¹M. A. Meitl, Z. T. Zhu, V. Kumar, K. J. Lee, X. Feng, Y. Y. Huang, I. Adesida, R. G. Nuzzo, and J. A. Rogers, *Nature Mater.* **5**, 33 (2006).

¹²H. Jiang, D. Y. Khang, J. Song, Y. Sun, Y. Huang, and J. A. Rogers, *Proc. Natl. Acad. Sci. U.S.A.* **104**, 15607 (2007).

¹³L. Siller, N. Peltakis, S. Krishnamurthy, Y. Chao, S. J. Bull, and M. R. C. Hunt, *Appl. Phys. Lett.* **86**, 221912 (2005).

¹⁴A. Bietsch and B. Michel, *J. Appl. Phys.* **88**, 4310 (2000).